Fixed Base Modal Survey of the MPCV Orion European Service Module Structural Test Article

James P. Winkel, James C. Akers, Vicente J. Suarez, and Lucas D. Staab
NASA Glenn Research Center
21000 Brookpark Road
Cleveland, Ohio 44135

Kevin L. Napolitano
ATA Engineering, Inc.
13290 Evening Creek Drive South, Suite 250
San Diego, California 92128

ABSTRACT

In 2016, the Orion European Service Module Structural Test Article (E-STA) underwent sine vibration testing using the multi-axis shaker system at NASA Glenn Research Center's (GRC) Plum Brook Station (PBS) Space Power Facility (SPF) Mechanical Vibration Facility (MVF). An innovative approach using measured constraint shapes at the interface of E-STA to the MVF Table allowed high-quality fixed base modal parameters of the E-STA to be extracted, which have been used to update the E-STA finite element model (FEM), without the need for a traditional fixed base modal survey. This innovative approach provided considerable program cost and test schedule savings. This paper documents this modal survey, which includes the modal pretest analysis sensor selection, the fixed base methodology using measured constraint shapes as virtual references and measured frequency response functions, and post-survey comparison between measured and analysis fixed base modal parameters.

Keywords: modal testing, vibrations, base-shake, environmental testing, fixed base, constraint shapes

INTRODUCTION

The Mechanical Vibration Facility (MVF), which is part of NASA Glenn Research Center's (GRC) Plum Brook Station (PBS) Space Power Facility (SPF) a three-axis vibration system that applies vibration in the vertical axis or two lateral orthogonal axes individually (not simultaneously) without the need of reconfiguration of the test article which saves testing cost and schedule and reduces risk to the test article. MVF was designed to perform sine vibration testing of a Multi-Purpose Crew Vehicle (MPCV) Orion-class spacecraft with a total mass of 75,000 lb, center of gravity (cg) height above the MVF Table of 284 in., and a diameter of 18 ft. The MVF Table, to which the E-STA was attached, is supported with 4 horizontal and 16 vertical actuators that are controlled with eight drive signals. MVF with the E-STA installed is shown in Figure 1.

The extraction of fixed base modes from structures mounted on shake tables has received a great deal of attention in recent year [1]-[6]. Difficulties arise, however, when the shake table motion is other than purely rigid body translation in the axis of the shake excitation, such as when the inertia forces imparted by the test article cause the shake table to rigid body motion (e.g. rocking and or elastic body motion (e.g. bending) at the combined system natural frequency rather than the test article fixed base natural frequency.

Currently, there are two promising methods to account for shake table motion. The first, developed by Sandia National Laboratories, is a transformation of measured modes to fixed base modes [7], and the second, developed by ATA Engineering, uses shake table accelerations as references when calculating Frequency Response Functions (FRFs) [8]. The key element in both methods is using a small number of shapes that adequately describe shaker table motion.

Figure 1. E-STA mounted on the MVF Table.

To meet the cost and schedule constraints of the E-STA Sine Vibration Test, it was determined that a fixed base modal survey of the E-STA could be performed using MVF utilizing the second method, which incorporates constraint shapes as references when calculating the FRFs, which has previously been documented [9] and includes the overall procedure for calculating FRFs. This paper documents the modal survey of the E-STA while mounted on the MVF Table. It includes the modal pretest analysis sensor selection, the fixed base methodology using measured constraint shapes as virtual references and measured FRFs, and post-survey comparison between measured and analysis fixed base modal parameters.

PRETEST ANALYSIS OBJECTIVES

The E-STA Sine Vibration Test campaign had three main objectives that are summarized below.

The first main objective was to verify the structural integrity of the European Service Module (ESM) under dynamic loading. These qualification loads were initially defined to be 1.25 times higher than the dynamic limit loads defined in the Orion-level coupled loads analysis (CLA). It should be noted that this first main objective was the primary driver of where the instrumentation on the vehicle was located and not the identification of modal parameters.

The second main objective of the test was to measure FRFs of the ESM equipment with respect to the base acceleration, to be used to validate the CLA results.

The third main objective of the testing, and the subject of this paper, was to identify the E-STA fixed base modal parameters of the primary target modes for both the fully filled propellant tank and partially filled propellant tank configurations. The primary target modes were identified by the European Space Agency (ESA) in conjunction with Airbus as the first six high-effective-mass modes whose shapes can be described as the first and second bending modes in the two lateral directions, the first axial torsion mode, and the first axial mode. Two additional important secondary structure modes were also included in the primary target mode set. Furthermore, a set of fourteen secondary target modes localized to the propellant tanks, solar array support structure, and other localized secondary structures was selected to help assist with the finite element model (FEM) correlation. It was understood from the start that these secondary modes would likely not be able to be validated by traditional means (cross-Modal Assurance Criteria (MAC) and cross-orthogonality, etc.) because of the constraints on sensor location. The modal effective mass table of the uncorrelated fully filled propellant tank configuration E-STA FEM is shown in Figure 2.

			Modal Effective Mass %						
	Mode #	Frequency	T1	T2	T3	R1	R2	R3	Mode Description (MPCV Coordinate System)
Primary Target Modes	1	3.37	0%	0%	75%	0%	97%	0%	First Stack Bending Mode Along Z Axis
	2	3.74	0%	86%	0%	0%	0%	92%	First Stack Bending Mode Along Y Axis
	3	6.52	0%	0%	15%	1%	0%	0%	Second Bending Mode Along Z Axis
	4	7.57	0%	0%	0%	72%	0%	0%	Torsion Mode
	5	7.84	0%	4%	0%	2%	0%	5%	Second Bending Mode Along Y Axis
	6	11.47	85%	0%	0%	0%	0%	0%	Axial Bounce Mode Along X Axis
	7	12.43	0%	0%	0%	0%	0%	0%	Important Secondary Structure Bending Mode Along Y Axis
	8	14.24	0%	0%	0%	0%	0%	0%	Important Secondary Structure Bending Mode Along Z Axis
Secondary Target Modes	9	15.16	0%	0%	0%	0%	0%	0%	Propellant Tanks Axial Modes
	10	16.13	0%	0%	0%	1%	0%	0%	
	11	16.41	4%	0%	0%	0%	0%	0%	
	12	17.29	0%	0%	0%	0%	0%	0%	
	13	18.24	1%	0%	0%	0%	0%	0%	Third Bending along Y Axis
	14	19.46	0%	0%	0%	0%	0%	0%	Propellant Tank Axial Modes
	15	20.75	0%	0%	0%	0%	0%	0%	
	16	22.47	0%	0%	0%	0%	0%	0%	RCS Modes
	17	22.53	0%	0%	0%	0%	0%	0%	
	18	22.72	0%	0%	0%	0%	0%	0%	Important Secondary Structure Torsion Mode
	19	23.03	0%	0%	0%	0%	0%	0%	Lateral Squeeze Mode
	20	23.92	0%	0%	0%	0%	0%	0%	Solar Array Secondary Structure Modes
	21	25.05	0%	0%	0%	0%	0%	0%	
	22	25.97	0%	0%	0%	0%	0%	0%	

Figure 2. E-STA full propellant tank configuration FEM modal effective mass (Uncorrelated Model).

PRETEST ANALYSIS SUMMARY

NASA GRC Structural Dynamics Branch (LMD) was tasked with determining the subset of existing sensors needed to support fixed base modal extraction of the target modes. NASA pretest goal is to have the cross-orthogonality should be greater than 90% on the diagonals and less than 10% off the diagonals. The frequency comparison between the TAM and FEM should also be less than 5%. The E-STA had a total of 736 accelerometers (i.e. test degrees of freedom [DOF], whose selection was based on measuring environments, but unfortunately were not optimally placed for modal parameter extraction. Unfortunately, no additional instrumentation could be added to the E-STA. The sensor down-selection was done using the fixed based E-STA fully filled propellant tank configuration FEM.

PRIMARY TARGET MODES TEST DOF SELECTION

Using all 736 test DOF would have been extremely cumbersome when extracting the fixed base modal parameters, and as expected, it was found to degrade the overall TAM results due to a significant amount of the instrumentation only capturing localized effects in the FEM. Engineers at GRC LMD developed a customized set of MATLAB-based test DOF selection tools that draw extensively upon ATA Engineering's IMAT® software packages. The overall sensor selection task was broken into two separate tasks. The first step in the process was to use the IMAT down-selection functionality to iterate through the full

736 DOF set. The program utilized the self-orthogonality (ORTHO) criteria to find the minimal test DOF set needed to clearly capture all primary target modes. A few additional test DOF were then added to meet the final cross-orthogonality and frequency comparison requirements between the test analysis model (TAM) and the full FEM (E-STA fully filled tank configuration) shapes. The primary target mode set only required 67 test DOF out of the full 736 DOF sensor set to adequately capture each mode independently. The TAM/FEM frequency comparison table and associated cross-orthogonality (XORTHO) for these 67 test DOF selected to optimize the extraction of the primary target modal parameters are shown in Figure 3. This minimal 67 test DOF set provides the basis for the second step in the process for determining additional test DOF that adequately capture the secondary target modes.

FEM/TAM Cross Orthogonality Table

TAM Shapes			FEM Shapes 1	2	3	4	5	6	7	8
	Oag		3.4	3.7	6.5	7.6	7.8	11.5	12.4	14.2
1	3.4		-1.00							
2	3.7			-1.00						
3	6.4				-1.00					
4	7.6					1.00				
5	7.8						-1.00			
6	11.9							1.00		
7	12.9								-0.99	-0.23
8	15.3								0.09	-0.94

FEM Mode	Freq (Hz)	TAM Mode	Freq (Hz)	%Difference
1	3.37	1	3.36	-0.49
2	3.74	2	3.70	-1.04
3	6.52	3	6.44	-1.17
4	7.57	4	7.57	0.01
5	7.84	5	7.80	-0.50
6	11.47	6	11.87	3.49
7	12.43	7	12.86	3.44
8	14.24	8	15.28	7.30

Figure 3. Minimal 67 test DOF TAM/FEM XORTHO (left), and TAM/FEM frequency comparison (right).

SECONDARY TARGET MODES TEST DOF SELECTION

When the same down selection procedure was applied to expand the test DOF to capture the fourteen secondary target modes, the program had a much more difficult time, in part because the secondary target modes were localized and had almost no modal effective mass. Based on past experience, this issue can usually be overcome by additional well-placed test DOF. However, in this case none of the E-STA test DOF were in locations that would adequately differentiate one secondary target mode from another.

The solar array secondary structure modes are a good example of this. Over eight of the fourteen secondary target modes had significant solar array structure translation and rotation. Of the four solar arrays on the vehicle, only one was flight like. The other three were mass simulators, each of which only had one triaxial accelerometer in the middle of the panel. Therefore, only translational motion could be measured on the three solar array mass simulators, leaving any rotation seen in the mode shapes unobservable by the measured DOF.

These two issues made the secondary test DOF set significantly larger and much less optimized. A modified approach using the down-selection program previously used for the primary target mode DOF set down-selection helped to ensure that the majority of the modal mass was captured in the TAM, but engineering judgment then had to be used to select DOF that adequately animated the mode shapes. The final cross-orthogonality between the TAM and FEM shapes did not meet the the pretest goal of greater than 90% on the diagonal and less than 10% on the off-diagonal. Hence, it was expected that the secondary target modes would be much more difficult to extract from the test data. The TAM/FEM frequency comparison table and associated cross-orthogonality for the 250 selected test DOF for the secondary target modes are shown in Figure 4).

MODAL SURVEY CONDUCT

As part of MVF performing a sine sweep, a low level random pretest characterization test run is performed with the 8 drive signals being uncorrelated so the MVF vibration controller can identify the dynamics of the integrated system and obtain a preliminary controller transfer function matrix. This random pretest was adapted to provide up to twenty minutes of low-level random base input excitation to the MVF Table from 2 Hz to 100 Hz while MVF was configured for vibration testing in the vertical direction. These random pretest acceleration time-history functions of the MVF Table responses were then processed to create up to eight independent constraint shape DOF that were then used as references when calculating FRFs.

FEM/TAM Cross Orthogonality Table

TAM Shapes		FEM Shapes																					
		1	2	3	4	5	6	7	8	9	10	11	12	13	14	15	16	17	18	19	20	21	22
	Oag	3.4	3.7	6.5	7.6	7.8	11.5	12.4	14.2	15.2	16.1	16.4	17.3	18.2	19.5	20.7	22.5	22.5	22.7	23.0	23.9	25.0	26.0
1	3.4	-1.00																					
2	3.7		-1.00																				
3	6.4			1.00																			
4	7.5				1.00																		
5	7.8					-1.00																	
6	11.7						1.00					0.11		0.08						-0.06			
7	12.9							0.99	0.23	0.05									-0.30				
8	15.2							-0.08	0.90	-0.43	-0.06		0.11			0.06		-0.06	0.43				
9	15.7							0.05	-0.34	-0.88	0.23	0.09	0.09						-0.36				
10	16.6								0.09	0.13	0.95	-0.22	-0.06						0.18				
11	17.2									-0.08	-0.17	-0.95	0.18		-0.17	0.08			-0.09				
12	18.6									0.08	0.05	0.13	0.90	0.35	-0.23								
13	19.0												0.34	-0.92	0.10					-0.05			
14	21.0											0.06	-0.12	-0.12	-0.95	0.08			-0.06				
15	22.5														0.06	0.98		0.10	-0.05		0.14		
16	24.3																0.94	0.28		0.20			
17	24.3																0.33	-0.86	-0.13	-0.37	0.07		
18	24.5															0.06	-0.07	-0.40		0.90			
19	24.8															-0.09		0.05	0.11		0.97	-0.14	-0.07
20	25.7																				0.11	0.99	
21	27.3																		0.56			0.05	0.16
22	27.9																						-0.87

FEM Mode	Freq (Hz)	TAM Mode	Freq (Hz)	%Difference
1	3.37	1	3.35	-0.54
2	3.74	2	3.70	-1.12
3	6.52	3	6.41	-1.69
4	7.57	4	7.54	-0.45
5	7.84	5	7.76	-1.05
6	11.47	6	11.75	2.46
7	12.43	7	12.85	3.38
8	14.24	8	15.22	6.88
9	15.16	9	15.74	3.86
10	16.13	10	16.60	2.91
11	16.41	11	17.24	5.07
12	17.29	12	18.62	7.66
13	18.24	13	18.97	3.97
14	19.46	14	20.97	7.76
15	20.75	15	22.54	8.63
16	22.47	16	24.25	7.94
17	22.53	17	24.33	7.99
18	22.72	21	27.33	20.32
19	23.03	18	24.51	6.44
20	23.92	19	24.80	3.66
21	25.05	20	25.71	2.64
22	25.97	22	27.95	7.63

Figure 4. 250 test DOF TAM/FEM XORTHO (top), and TAM/FEM frequency comparison (bottom).

CONSTRAINT SHAPE CALCULATION

A total of eight constraint shapes were considered because there were eight independent actuator groups attached to the MVF table and each driven with uncorrelated drive signal. A total of 36 accelerometers mounted to the MVF table were used to calculate the constraint shapes, and they are shown in Figure 5. The first six constraint shapes were the six rigid body modes of the MVF table. The final two constraint shapes were calculated by performing a singular value decomposition of the time history functions from 4 to 80 Hz generated by taking the 36 MVF Table accelerations and removing the contributions due to the rigid body motion of the MVF Table in a least-squares sense.

FREQUENCY RESPONSE FUNCTION CALCULATION

Since random time-history data was collected, several parameters were studied to determine which method would be the best for calculating the cleanest set of FRFs. These parameters included the number of references used, the FRF method (H_1 versus H_{SVD} [10]), and the FRF averaging method (Welch versus Daniell [11]). The final set of FRFs was based on using the following:

1. The first seven constraint shapes (six rigid body modes and first "potato chip" mode) as references.
2. H_{SVD} using seven constraint shapes and three accelerometers as basis vectors to capture peaks of primary modes

3. Welch method (Hanning window, 90% overlap)

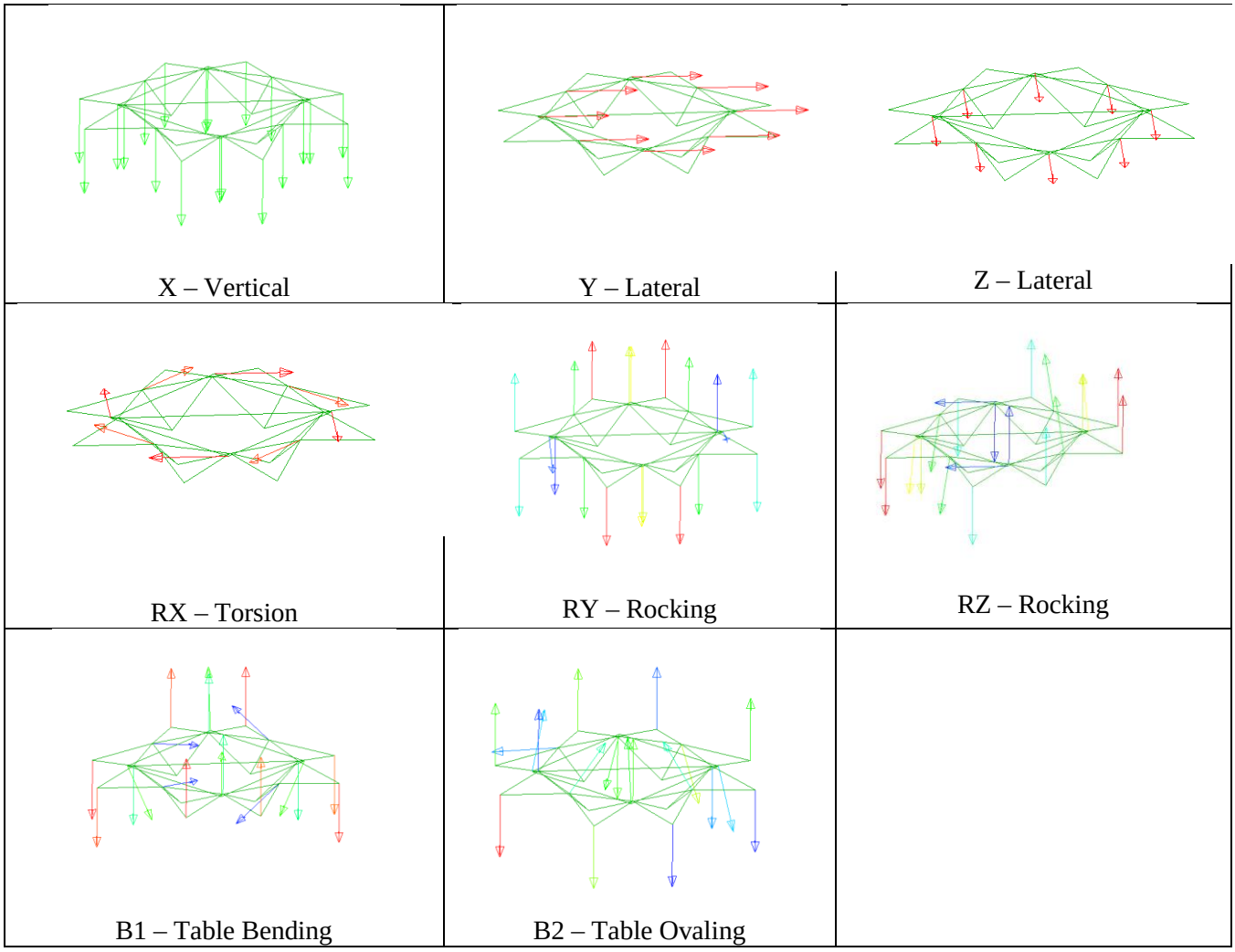

Figure 5. Constraint shapes.

A power spectrum mode-indicator function (PSMIF) of each reference is presented in Figure 6. The PSMIFs associated with rigid body motions are much cleaner than the PSMIF of the seventh reference (i.e. MVF Table bending B1), which is associated with flexible motion of the MVF Table. The eighth constraint shape, B2, which was dominated by ovaling of the MVF Table was not well excited because of the geometry of the actuators relative to this constraint shape and thus the shape was not used. The first six primary target modes were well excited by the rigid body motion of the MVF Table as evidenced by the associated strong peaks in the PSMIF. Upon closer inspection it can be seen that each of the primary target modes is excited by the appropriate MVF Table rigid body motion. For example, the primary torsion and axial target modes are excited by in-plane rotation and vertical motion of the MVF table, respectively. Note that the FRFs associated with two important secondary structure modes appear to be not well excited because they are heavily damped. This challenge is common in almost all modal surveys, and one solution is to connect modal shakers to the secondary structure and excite these modes directly. In this case, however, all primary target modes were able to be extracted from the random pretest test data.

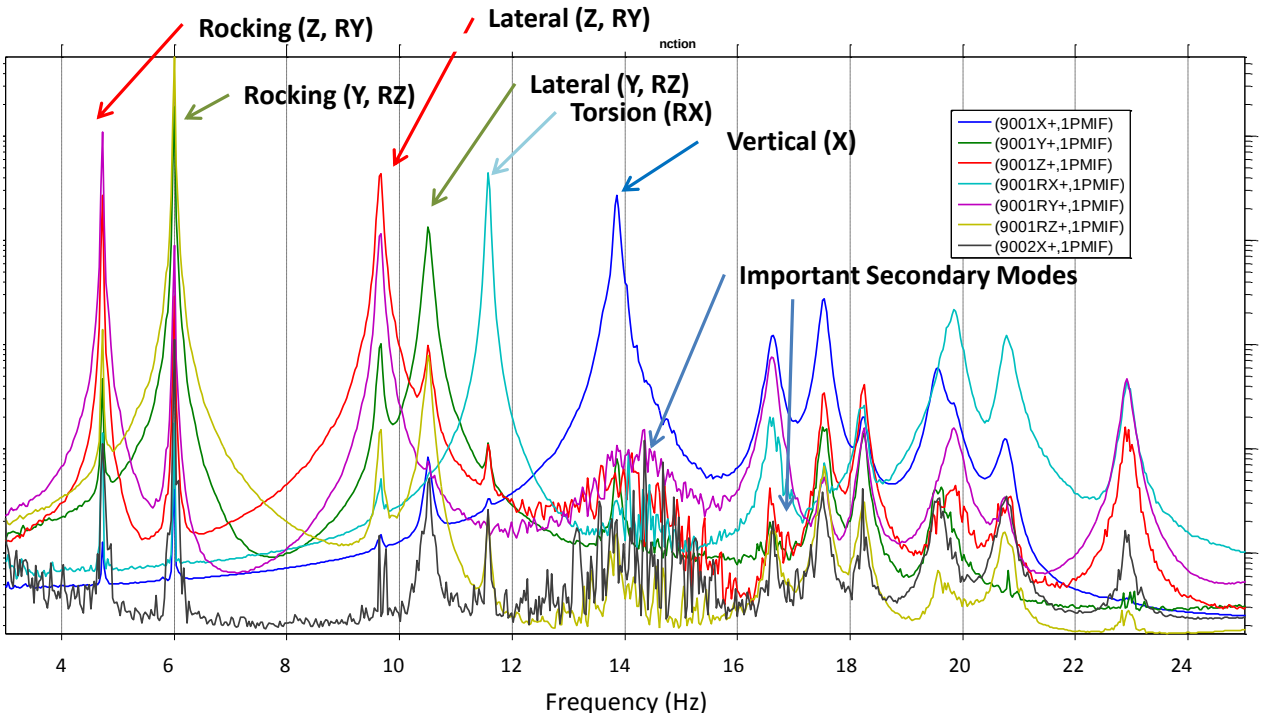

Figure 6. Power spectrum mode-indicator functions comparing response of all channels due to each constraint shape reference.

One check to determine the fixity of the MVF table is to look at the base motion compared to the motion of the accelerometers on the MVF table. This can be represented by overlaying a PSMIF of the test article accelerometers and a PSMIF of just the MVF Table accelerometers Figure 7. Ideally, the base motion should be constant as a function of frequency, but just as in conventional fixed base modal tests the base may not be perfectly fixed, leading to some small level of resonance amplification. The level of this amplification determines how accurate the fixed base modal frequencies are. In this case, the resonance amplification of the two primary bending modes is very small compared to the overall response and is nearly flat for all frequencies up to 50 Hz. Hence the modal parameters extracted are fixed base.

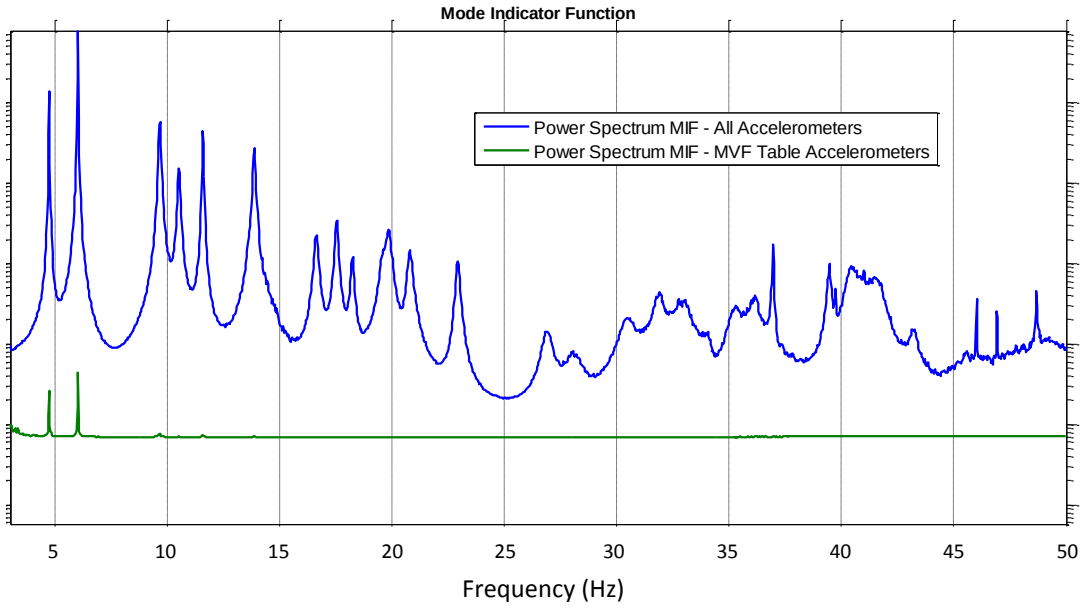

Figure 7. Power spectrum mode-indicator function comparing E-STA response to MVF Table response.

MODAL EXTRACTION

Fixed base modal parameters were then extracted from the fixed base FRFs just as they would be in any fixed base modal test. The FRFs associated with the first six rigid body constraint shapes as references were used to extract modal parameters for two reasons. The first is that the FRFs associated with rigid body motion were cleaner than the FRFs associated with constraint shape associated with flexible motion of the MVF Table, and the second is that the FRFs associated with the six rigid body shapes are guaranteed to excite high-effective-mass modes. A stability plot from ATA's IMAT AFPoly modal analysis tool, showing the pole estimates and overlays of the Complex Mode Indicator Functions (CMIF's), is shown in Figure 8. The well-defined "race track" pattern of the pole estimates and their alignment with the strong peaks in the CMIF aids in the modal extraction process.

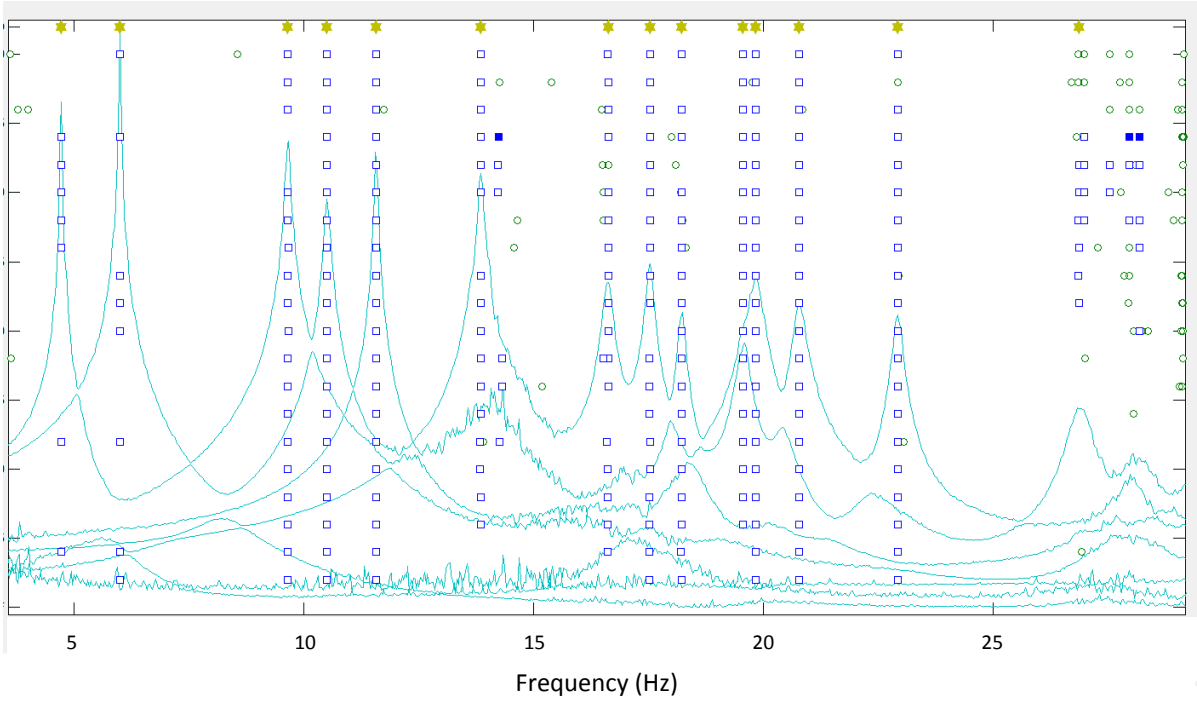

Figure 8. Example stability plot created using ATA's AFPoly modal analysis tool.

The extraction of the important secondary structure modes was difficult due to the fact that the linkages/connections are very nonlinear and resulted in very high damping levels. Specific FRFs associated with MVF Table constraint shape that clearly excited these modes and response DOF on the secondary structure were used with narrow-band modal analysis tools, such as ATA's IMAT SDOFIT tool, were used to extract these modes. One of these FRF showing the important secondary structure mode is shown in Figure 9. Note that because of the high damping, there is not a pronounced resonance peak in the FRF, but the phase angle roll off does indicate a mode is present.

The first two 1st lateral bending modes, 1st torsion, and 1st axial test-measured fixed base modes are shown in Figure 10. Base fixity was assessed by viewing MVF Table motion for each mode shape.

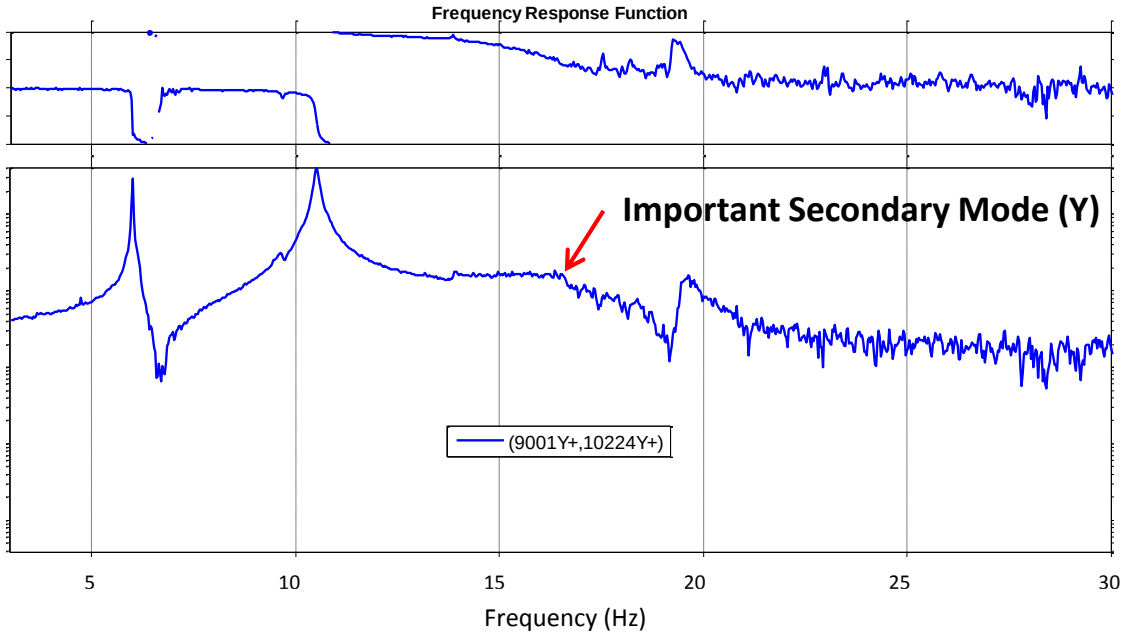

Figure 9. FRF associated with important secondary structure lateral (Y) motion and table lateral Y motion.

POST TEST ANALYSIS

After the fixed-base mode shapes were extracted, test ORTHO and test-analysis XORTHO were calculated to assess test mode quality Figure 11. Ideally, the off-diagonal terms of the test ORTHO should be below 10%. Higher off-diagonal terms may occur for a number of reasons, but in this case it appears that the 11% term is due to the important secondary structure lateral mode being very difficult to extract. The test-analysis XORTHO shows that all eight primary target modes were adequately captured.

A final check was performed to assess how many of the analysis modes were captured in the test by looking at the XORTHO between all extracted test shapes to all analysis shapes up to 26 Hz and is shown in Figure 12. Overall, there is mostly a one-to-one match between a given test shape and a given analysis shape, although in some cases multiple test modes capture a given analysis mode. This can be assessed by looking at the "CRSS 3%" and the "CRSS All" rows at the bottom of the table. The "CRSS 3%" row describes how much of the analysis mode is captured by all test modes within 3% in frequency of the test mode that best maps to the analysis mode. The "CRSS All" row describes how much of each analysis mode is captured by all of the test shapes.

The only analysis mode that does not have a significant match to a single test mode is analysis mode 18, which is the important secondary structure's 1st torsion mode. The XORTHO indicates that this mode lies in the 32–34 Hz range, and this assessment was verified by looking at the FRFs associated with secondary structure tangential accelerometers due to a torsional input of the MVF Table (9001RX+), which is shown in Figure 13. There is a heavily damped mode where both accelerometers are in phase, as they should be for a torsion mode, near 33 Hz. Note that the phase change near this frequency is more than 180 degrees, which means that there are multiple modes present.

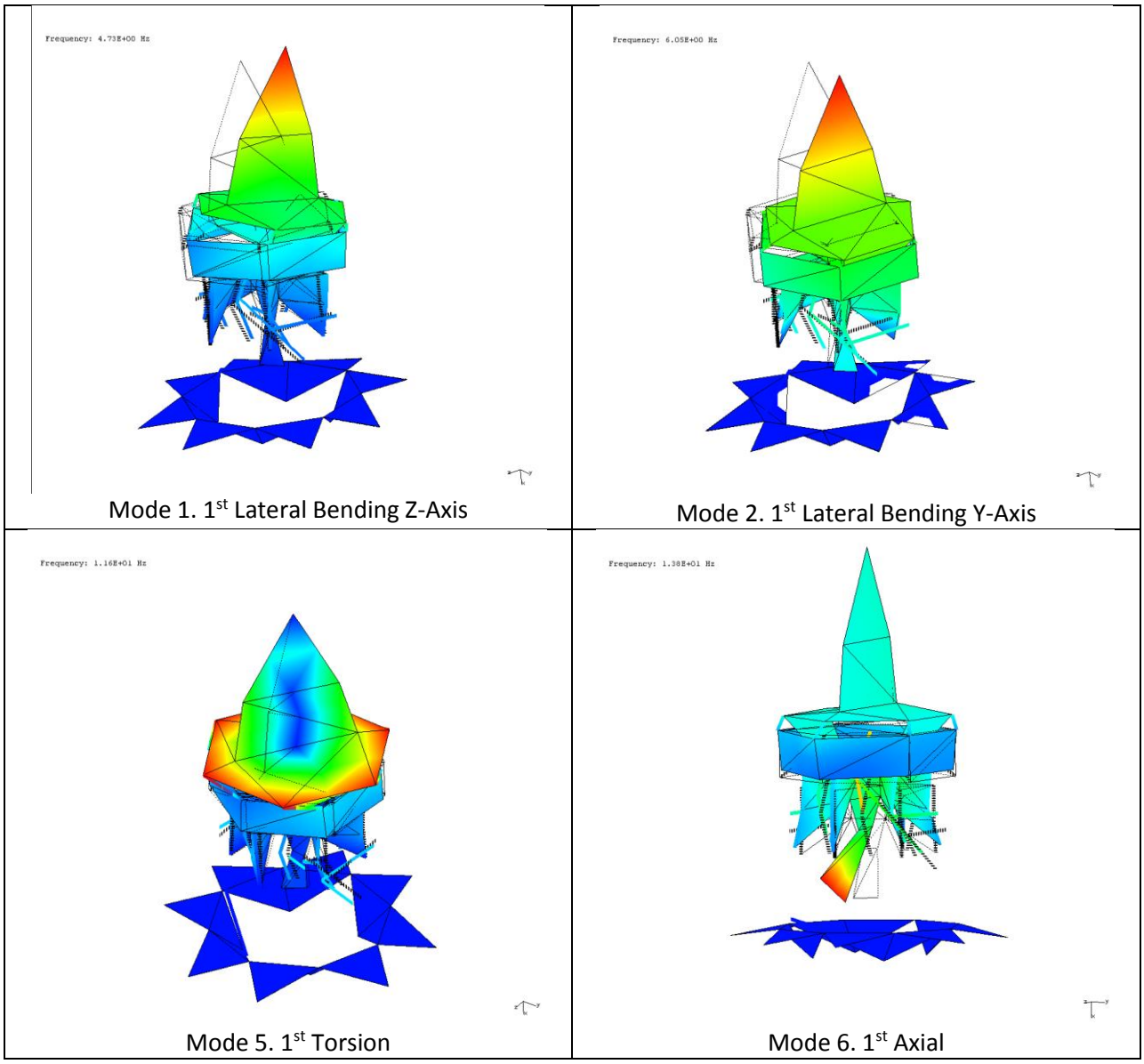

Figure 10. Example primary target fixed base test mode shapes.

Test Self Orthogonality Table

			Test Shapes							
			1	2	3	4	5	6	7	8
		Ott	4.7	6.1	9.7	10.5	11.6	13.8	14.2	16.3
Test Shapes	1	4.7	1.00							
	2	6.1		1.00						
	3	9.7			1.00					
	4	10.5				1.00				0.07
	5	11.6					1.00			
	6	13.8						1.00		0.11
	7	14.2							1.00	0.05
	8	16.3				0.07		0.11	0.05	1.00

FEM/Test Cross Orthogonality Table

			FEM shapes							
			1	2	3	4	5	6	7	8
		Otg	3.4	3.7	6.5	7.6	7.8	11.5	12.4	14.2
Test Shapes	1	4.7	0.97		0.23					
	2	6.1		0.97						
	3	9.7	0.23		0.96					
	4	10.5					0.97			
	5	11.6				0.91				
	6	13.8						0.98		
	7	14.2							0.21	0.96
	8	16.3						0.21	0.75	

Figure 11. Primary target mode test shape ORTHO (left), and test-analysis XORTHO (right)

FEM/Test Cross Orthogonality Table

FEM shapes

Test Shapes		Otg	1	2	3	4	5	6	7	8	9	10	11	12	13	14	15	16	17	18	19	20	21	22
			3.4	3.7	6.5	7.6	7.8	11.5	12.4	14.2	15.2	16.1	16.4	17.3	18.2	19.5	20.7	22.5	22.5	22.7	23.0	23.9	25.0	26.0
	1	4.7	0.97		0.23																			
	2	6.1		0.97																				
	3	9.7	0.23		0.96																			
	4	10.5					0.97																	
	5	11.6				0.91					0.22	0.30												
	6	13.8						0.98																
	7	14.2							0.21	0.96										0.41				
	8	16.3						0.21	0.75		0.36	0.22	0.34							0.37				
	9	16.6								0.26	0.88	0.34												
	10	17.5						0.23					0.93											
	11	18.2										0.41		0.84	0.29									
	12	19.6													0.87	0.44								
	13	19.8				0.27					0.32	0.70		0.40		0.37								
	14	20.8				0.21						0.39			0.33	0.77								
	15	22.9															0.96							
	16	26.9																0.53	0.24			0.77		
	17	27.0																0.72	0.21			0.61	0.21	
	18	27.5																0.32	0.84		0.30			
	19	28.0																			0.92			
	20	28.2																			0.39	0.23	0.82	
	21	30.5																						0.77
	22	31.9																						
	23	32.4																		0.24				
	24	32.7																		0.27				0.32
	25	33.0																		0.21				
	26	34.0							0.22	0.24										0.50				
FEM	CRSS 3%		0.97	0.97	0.96	0.91	0.97	0.99	0.86	0.97	0.88	0.70	0.93	0.84	0.88	0.77	0.96	0.98	0.98	0.54	0.93	0.94	0.94	0.77
FEM	CRSS All		1.00	1.00	1.00	0.98	1.00	1.00	0.99	1.00	1.00	1.00	1.00	1.00	1.00	1.00	1.00	1.00	0.99	0.95	0.98	0.98	0.99	0.89

Figure 12. XORTHO of all extracted test shapes versus all analysis shapes to 26 Hz.

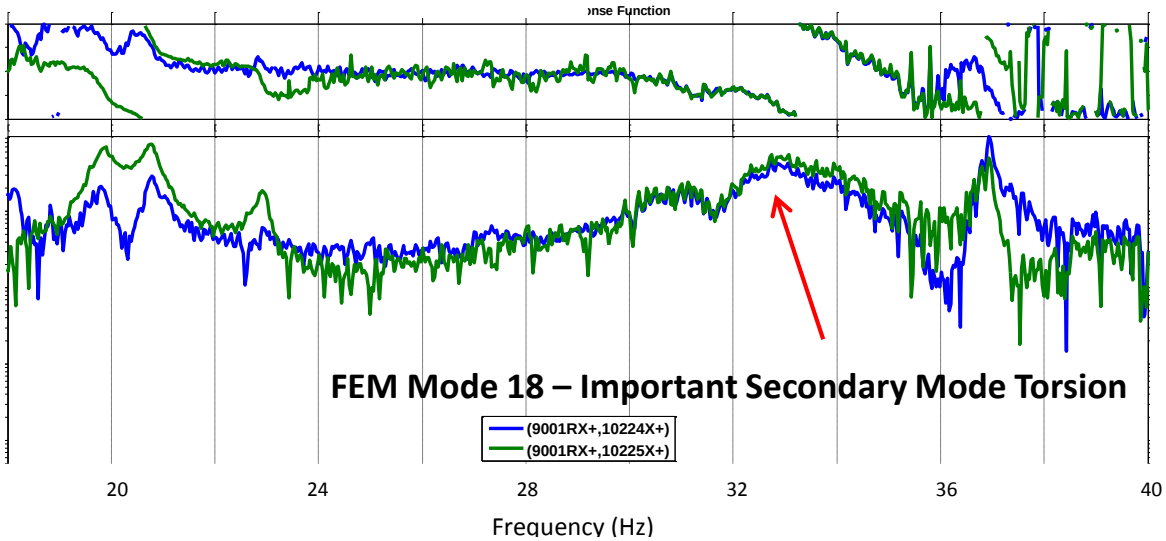

Figure 13. FRFs associated with tangential motion and table in-plane rotational input.

SUMMARY

This paper presents the results of the modal survey of the E-STA mounted on the MVF table during the E-STA Sine Vibration Test. In spite of the challenges associated with this test, such as a non-optimal candidate sensor set and a dynamically flexible MVF Table, high quality fixed-base modes were extracted for the eight primary target modes using innovative techniques to down-select to appropriate sensor sets and to calculate fixed base FRFs.

The fixed base FRFs were calculated using seven constraint shapes of the MVF Table, which included the six rigid body motions and one flex motion. Once these FRFs were calculated, standard modal analysis techniques were used to extract fixed base modes of the test article. The test was deemed a success since all analysis modes up to 26 Hz, including the eight primary target modes, were captured as much as practicable given the sensor location constraints.

REFERENCES

[1] Carne, T.G., D.R. Martinez, and A.R. Nord. "A Comparison of Fixed-Base and Driven Base Modal Testing of an Electronics Package." *Proceedings of the Seventh International Modal Analysis Conference*, 1989: 672–9.

[2] Beliveau, J.G., F.R. Vigneron, Y. Soucy, and S. Draisey. "Modal Parameter Estimation from Base Excitation." *Journal of Sound and Vibration* 107. 1986: 435–49.

[3] Fullekrug, U. "Determination of Effective Masses and Modal Masses from Base-Driven Tests." *Proceedings of the 14th International Modal Analysis Conference*, 1996: 671–81.

[4] Sinapius, J.M. "Identification of Fixed and Free Interface Normal Modes by Base Excitation." *Proceedings of the 14th International Modal Analysis Conference*, 1996: 23–31.

[5] Mayes, R.L., and L.D. Bridgers. "Extracting Fixed Base Modal Models from Vibration Tests on Flexible Tables." *Proceedings of the 27th International Modal Analysis Conference*, 2009.

[6] Napolitano, K., and N. Yoder. "Fixed Base FRF Using Boundary Measurements as References – Analytical Derivation." *Proceedings of the 30th International Modal Analysis Conference*, 2012.

[7] Mayes, R., D. Rohe, and J. Blecke. "Extending the Frequency Band for Fixed Base Modal Analysis on a Vibration Slip Table." *Proceedings of the 31th International Modal Analysis Conference*, 2013.

[8] Napolitano, K., and N. Yoder. "Extraction of Fixed-Base Modes of a Structure Mounted on a Shake Table." *Proceedings of the 31th International Modal Analysis Conference*, 2013.

[9] Staab, L., J. Winkel, J. Suárez, T. Jones, and K. Napolitano. "Fixed Base Modal Testing Using the Mechanical Vibration Facility 3-Axis Base Shake System." *Proceedings of the 34th International Modal Analysis Conference*, 2016.

[10] Napolitano, K. "Using Singular Value Decomposition to Estimate Frequency Response Functions." *Proceedings of the 34th International Modal Analysis Conference*, 2016.

[11] Daniell, P. "Discussion of 'On the Theoretical Specification and Sampling Properties of Autocorrelated Time-Series.'" *Journal of the Royal Statistical Society* 8, 88–90.